



Effects of hunger, satiety and oral glucose on effective connectivity between hypothalamus and insular cortex



Arkan Al-Zubaidi^{a,b,**}, Sandra Iglesias^c, Klaas E. Stephan^c, Macià Buades-Rotger^a,
 Marcus Heldmann^{a,d}, Janis Marc Nolde^a, Henriette Kirchner^e, Alfred Mertins^f,
 Kamila Jauch-Chara^g, Thomas F. Münte^{a,d,*}

^a Department of Neurology, University of Lübeck, Lübeck, Germany

^b Applied Neurocognitive Psychology Lab, University of Oldenburg, Oldenburg, Germany

^c Translational Neuromodeling Unit, Institute for Biomedical Engineering, University of Zurich & ETH Zurich, Zurich, Switzerland

^d Institute of Psychology II, University of Lübeck, Lübeck, Germany

^e Department of Internal Medicine I, University of Lübeck, Lübeck, Germany

^f Institute for Signal Processing, University of Lübeck, Lübeck, Germany

^g Department of Psychiatry and Psychotherapy, Christian-Albrechts-University, Kiel, Germany

ARTICLE INFO

Keywords:

Prandial states
 Glucose administration
 Resting-state fMRI
 Spectral DCM
 Effective connectivity
 Interoception

ABSTRACT

The hypothalamus and insular cortex play an essential role in the integration of endocrine and homeostatic signals and their impact on food intake. Resting-state functional connectivity alterations of the hypothalamus, posterior insula (PINS) and anterior insula (AINS) are modulated by metabolic states and caloric intake. Nevertheless, a deeper understanding of how these factors affect the strength of connectivity between hypothalamus, PINS and AINS is missing. This study investigated whether effective (directed) connectivity within this network varies as a function of prandial states (hunger vs. satiety) and energy availability (glucose levels and/or hormonal modulation). To address this question, we measured twenty healthy male participants of normal weight twice: once after 36 h of fasting (except water consumption) and once under satiated conditions. During each session, resting-state functional MRI (rs-fMRI) and hormone concentrations were recorded before and after glucose administration. Spectral dynamic causal modeling (spDCM) was used to assess the effective connectivity between the hypothalamus and anterior and posterior insula. Using Bayesian model selection, we observed that the same model was identified as the most likely model for each rs-fMRI recording. Compared to satiety, the hunger condition enhanced the strength of the forward connections from PINS to AINS and reduced the strength of backward connections from AINS to PINS. Furthermore, the strength of connectivity from PINS to AINS was positively related to plasma cortisol levels in the hunger condition, mainly before glucose administration. However, there was no direct relationship between glucose treatment and effective connectivity. Our findings suggest that prandial states modulate connectivity between PINS and AINS and relate to theories of interoception and homeostatic regulation that invoke hierarchical relations between posterior and anterior insula.

1. Introduction

Food intake in humans is determined and affected by non-homeostatic (i.e. external) factors, such as the social situation and time, and homeostatic (i.e. internal) factors related to the body's energy needs, such as hunger and starvation (Begg and Woods, 2013; Woods, 2009; Woods and Ramsay, 2011). However, controlling food intake and energy homeostasis under different metabolic, i.e. prandial states

(hunger vs. satiety), is remarkably complex in humans since it is influenced by the interaction of the endocrine system and brain structures involved in monitoring interoceptive signals (Begg and Woods, 2013; De Silva et al., 2012; Mayer, 2011). Interactions between brain function and body energy homeostasis can be further altered by various pathophysiological conditions such as increased blood lipids in obesity (Murray et al., 2014; Morton et al., 2014; Val-Laillet et al., 2015). For instance, in overweight subjects, body mass index (BMI) and insulin levels are associated with variations in resting-state functional connectivity (FC) after

* Corresponding author. Department of Neurology, University of Lübeck, Ratzeburger Allee 160, 23538, Lübeck, Germany.

** Corresponding author. Applied Neurocognitive Psychology Lab, University of Oldenburg, Oldenburg, Germany

E-mail addresses: arkan.al-zubaidi@uni-oldenburg.de (A. Al-Zubaidi), thomas.muente@neuro.uni-luebeck.de (T.F. Münte).

<https://doi.org/10.1016/j.neuroimage.2020.116931>

Received 4 April 2019; Received in revised form 12 April 2020; Accepted 7 May 2020

Available online 14 May 2020

1053-8119/© 2020 The Author(s). Published by Elsevier Inc. This is an open access article under the CC BY license (<http://creativecommons.org/licenses/by/4.0/>).

Abbreviations	
AAL	Automated-Anatomical-Labeling
AINS	anterior insula
ANOVA	analysis of variance
BMI	body mass index
BMS	Bayesian model selection
BOLD	blood oxygen level dependent
CFS	cerebrospinal fluid
CSD	cross-spectra density
DARTEL	diffeomorphic anatomical registration through exponentiated Lie algebra
DCM	dynamic causal modeling
DPARSFA	data processing assistant for resting-state fMRI advanced edition
EC	effective connectivity
FC	functional connectivity
GLM	general linear model
LH	lateral hypothalamus
LAINS	left anterior insula
LPINS	left posterior insula
LME	linear mixed-effects
MLR	multiple linear regression
NPCs	neuronal parameter components
NPEs	neuronal parameter estimates
PCs	principal components
PCA	principal component analysis
RAINS	right anterior insula
RPINS	right posterior insula
PINS	posterior insula
rmANOVA	repeated measures ANOVA
rs-fMRI	resting-state functional magnetic resonance imaging
ROI	regions of interest
SCD	singular value decomposition
spDCM	spectral DCM
TE	echo time
TR	repetition time
VMN	ventromedial hypothalamus nucleus

an overnight fast (Kullmann et al., 2012). Furthermore, FC imbalance between brain regions associated with impulsivity (i.e. inferior parietal lobe), response inhibition (i.e. frontal pole) and reward (i.e. nucleus accumbens) is correlated with increased food approach behaviors and obesity in children (Chodkowski et al., 2016). Nevertheless, FC captures purely correlational relationships between regions and does not yield information about the direction of influences. Therefore, studying how the directed connectivity within brain networks involved in homeostatic regulation is modulated by physiological (prandial) states constitutes an important step forward to understand the neural control of food intake.

Both the hypothalamus and insular cortex respond to hunger- and satiety-inducing signals (Mayer, 2011; Schloegl et al., 2011; Valassi et al., 2008; Wright et al., 2016). For instance, whilst hunger increases activity of the hypothalamus (Lizarbe et al., 2013), satiety exerts suppressive effects on the hypothalamic signal, as occurs after exogenous glucose or insulin administration, (Kullmann et al., 2013; Little et al., 2014; Smeets et al., 2007, 2005; Thomas et al., 2015). However, most brain imaging studies used a typical resting-state fMRI (rs-fMRI) approach to investigate the FC between seeds (i.e. hypothalamus, AINS and PINS) and brain areas involved in appetite regulation (Cauda et al., 2011; Frank et al., 2013; Moreno-Lopez et al., 2016; Wright et al., 2016) and thus cannot clarify the directionality of connections between these regions. For example, a study using seed-based analysis to investigate the effect of fasting and satiation on FC in healthy subjects found an enhancement of FC between the posterior insula and superior frontal gyrus, and between the hypothalamus and inferior frontal gyrus after overnight fasting (Wright et al., 2016).

Much of our understanding on how the central nervous system governs ingestive behavior is based on experiments in rodents, which has proven especially fruitful to uncover functional sub specializations within the hypothalamus (Timper and Brüning, 2017). However, the markedly larger and more gyrified neocortex observed in humans (Sun and Hevner, 2014) complicates direct comparisons in cortical processing between humans and rodents. Non-human primates offer a more valid animal model with which to delineate the neural architecture of appetite regulation. Indeed, convergent evidence from studies in non-human and human primates suggests a highly conserved architecture underlying the neural processing of food. Specifically, the AINS –which contains the primary gustatory cortex–appears to code for the physical properties of food (i.e. texture, temperature), whereas the orbitofrontal cortex (OFC) tracks the subjective pleasantness of flavors and smells (Rolls, 2006). Subcortical areas such as the hypothalamus or the brain stem do not seem to be involved in these evaluative processes to the same degree. Rather,

these structures receive interoceptive information signaling hunger and satiety (DelParigi et al., 2005; Pelchat et al., 2004; Rolls, 2006). This information is then relayed through the PINS towards the AINS and from there to orbitofrontal areas, where subjective valuation of the organisms' metabolic state presumably takes place (Craig, 2014, 2005; Dagher et al., 2017).

Recent computational theories of interoception have proposed hierarchically structured network models (Seth, 2013) that include reciprocal connections between hypothalamus, posterior insula and anterior insula (e.g., see Fig. 7 in Stephan et al., 2016 and Fig. 3 in Manjaly et al., 2019). These theories make predictions about patterns of effective connectivity that are of relevance for the present study. Specifically, these theories predict that in states of dyshomeostasis (such as hunger), forward or ascending connections (which are assumed to signal deviations between actual and expected bodily states, i.e. prediction errors) are enhanced. Conversely, in states of homeostasis (such as satiation), forward connectivity should be reduced, relative to backward or descending connections (which are thought to transmit predictions about bodily states).

Finally, it is unclear how prandial states affect the effective connectivity (EC) between these regions. To fill this research gap, we applied dynamic causal modeling (DCM; Friston et al., 2003) to infer effective (directed) connectivity on latent (hidden) neuronal states from measured brain data in a study that manipulated prandial state (hunger vs. satiety) and energy availability (before and after glucose administration) in healthy young men. DCM can be used to gather evidence favoring one network model (hypothesis) over other models and to understand how nodes (i.e. brain regions) might influence each other (Friston et al., 2011). A recent DCM variant called spectral DCM (spDCM) estimates EC from the intrinsic signal fluctuations present in rs-fMRI data (Friston et al., 2014). Spectral DCM uses a variational Bayesian procedure to estimate the strengths of endogenous connectivity in the absence of (known) external perturbations like tasks or stimuli.

The current data-set has been used in a previous publication, in which we reported reduced FC of AINS after glucose application during both hunger and satiety (Al-Zubaidi et al., 2018). Furthermore, we found that increases in plasma insulin levels between hunger and satiety were negatively related to PINS activity after glucose administration (Al-Zubaidi et al., 2019).

In the present investigation, we first used spDCM to estimate the EC parameters for each participant and experimental condition (hunger vs. satiety, before vs. after glucose administration) using rs-fMRI data. Subsequently, we applied Bayesian model selection (BMS; Stephan et al.,

2009) to determine the most plausible model in each condition from a set of competing hypotheses (i.e. models). Finally, we performed an analysis of variance (ANOVA) on estimated neural parameters to test whether the estimated connection strengths between hypothalamus, PINS and AINS are affected by the prandial states and glucose treatment.

For the present analysis, it might be expected that increased forward connectivity in the hypothalamus-PINS-AINS network during fasting relative to satiety, in line with studies showing enhanced hypothalamic activity (Lizarbe et al., 2013) and coupling with frontal structures (Wright et al., 2016) in a hunger state. We further speculated that glucose administration would act as a transient satiety signal (Kullmann et al., 2013; Little et al., 2014; Smeets et al., 2007, 2005; Thomas et al., 2015) and hence reduce the strength of these forward connections. By contrast, predictions regarding the effect of prandial state and glucose administration on backward connections are less straightforward because, in the computational theories mentioned above, different backward connections have slightly different functions and depend on context. For example, backward connections between insular areas are thought to carry predictive signals that serve perceptual updating (and are thus thought to change between hunger and satiation), whereas backward connections from cortical visceromotor regions like anterior insula towards effector regions such as the hypothalamus are assumed to carry predictive signals which change homeostatic setpoints but are only invoked in certain contexts (Stephan et al., 2016).

2. Experimental procedures and methods

2.1. Participants

The study was carried out in accordance with the Declaration of Helsinki (2002) and was approved by the ethics committee of the University of Lübeck, Germany.

Twenty-four healthy male volunteers (mean age 25 ± 5 years) with a BMI within the normal range (mean BMI 22.5 ± 2.5 kg/m²) gave oral and written informed consent before participating in our study. All participants were subjected to a medical interview and were excluded from participation when reporting any drug consumption, somatic (e.g., diabetes, metabolic syndrome) or mental health disorders (e.g., depression disorder, eating disorders) in the present or past. Participants were financially compensated. In four subjects, we were not able to obtain a sufficient normalization of the functional individual brain image into standard space. Accordingly, these subjects were excluded from the analyses (see section “Region-of-interest time-series extraction” for further explanation).

2.2. Experimental design

Participants were examined twice, one time in the hunger condition and the other time after receiving regular standardized meals. The participants underwent these conditions in a randomized order. Each session lasted two days with sessions scheduled exactly one week apart. On the second day of each session at 1:05 p.m., functional resting-state MRI was recorded. Participants were instructed to close their eyes, to lie as still as possible and to avoid any particular cognitive activity. At 1:25 p.m., after completing the first resting-state recording lasting for 6 min, participants drank a water solution containing the equivalent of 75 g glucose. At 1:45 p.m., 20 min after the oral glucose intake, a second resting-state recording was obtained (6 min). Also, 19 blood samples per subject and condition were collected, of which 13 samples were drawn before and six samples after glucose administration. Fig. 1 shows the time course of the mean concentrations of plasma glucose, insulin and cortisol on the second day of the experiment for hunger and satiety conditions. In each condition, participants rated their subjective hunger feeling 20 min before and 20 min after oral glucose intake with a visual analog scale ranging from zero (not hungry at all) to nine (very hungry). The details of the type of meals, the timing of collecting blood samples and image

acquisition parameters can be found in the supplementary material. This information is also reported in detail in Al-Zubaidi et al. (2018).

2.3. Handling and analyses of blood samples and hunger ratings

Glucose concentrations were determined using the B-Glucose-Data-Management device (HemoCue GmbH, Grossostheim, Germany). For measuring the hormone levels, blood samples were centrifuged immediately. The supernatants were stored at -80 °C until they were analyzed. Blood serum and plasma were used to measure the insulin and cortisol levels by commercial enzyme-linked immunoassay (Immulate DPC, Los Angeles, USA; insulin: intra-assay coefficient of variation (CV)

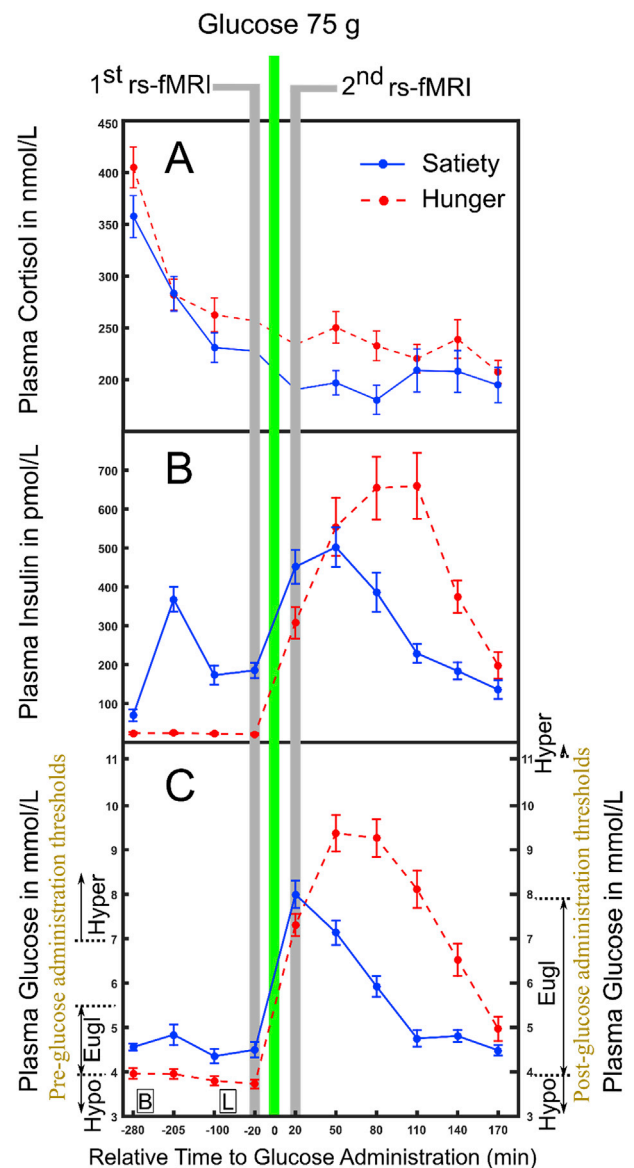


Fig. 1. Time course of the mean blood plasma concentrations for cortisol (A), insulin (B) and glucose (C) under hunger and satiety conditions before and after oral glucose treatment (time point 0). Boxes on the bottom of the graph indicate the time points of meals on the second day (B = breakfast, L = lunch at 09:00 a.m. and 12:00 p.m., respectively). In each condition, the first rs-fMRI was recorded 20 min before, the second rs-fMRI 20 min after the intake of oral glucose. The black dashed lines on y-axis of the Figure (C) refer to hypoglycemia (Hypo), euglycemia (Eugly) and hyperglycemia (Hyper) ranges for fasting glucose levels pre- (left y-axis) and post-glucose administration (right y-axis, at 120 min after glucose administration). The two lower panels are adapted from Al-Zubaidi et al. (2019). Figure C is adapted from Al-Zubaidi et al. (2018).

< 1.5% and inter-assay CV < 4.9%; cortisol: intra-assay CV < 1.7% and inter-assay CV < 2.8%).

To investigate differences between the two experimental conditions (hunger and satiety) for plasma glucose, insulin and cortisol levels before and after glucose administration (oral glucose intake) two averages across the relevant samples of the second day were calculated for each participant and condition: one before and one after the oral glucose intake.

To test for differences, two-way repeated-measures ANOVAs (rmANOVA) with factors prandial state (levels: hunger, satiety) and glucose administration (levels: before, after glucose intake) were performed for each of the dependent variables, i.e. hunger rating, plasma glucose, insulin, and cortisol levels, separately. All analyses were performed using SPSS software Version 22.0. Values are reported as mean (M) and standard deviation (\pm SD). Also, we included partial eta squared (η_p^2) as a measure of the effect size of the performed rmANOVAs.

2.4. Preprocessing

Preprocessing of the data was performed with the “data processing assistant for resting-state fMRI” toolbox (DPARSF advanced edition, version 3.2, available at <http://rfmri.org/DPARSF>). DPARSF uses a subset of functions provided by SPM (SPM12, available at <http://www.fil.ion.ucl.ac.uk/spm/>). The rs-fMRI images were preprocessed as follows: (i) The first 7 vol of each dataset were discarded to allow the signal to reach equilibrium and to allow the subjects to adjust to the scanning noise; (ii) The origins of structural and functional images were manually set to the anterior commissure and reoriented to enable a better alignment to the SPM template in order to prevent normalization errors and to optimize between-subject alignment; (iii) Functional images were slice-time corrected to the middle slice by means of Fourier phase shift interpolation (Sladky et al., 2011). Head movement correction was performed on data by volume-realignment to the mean volume using a rigid body spatial transform to estimate the realignment parameters; (iv) Then, the T1 structural image was co-registered to the mean functional image of each subject; (v) Gray matter, white matter and cerebrospinal fluid (CSF) segmentation, bias correction and spatial normalization of the T1 structural image were adjusted to the Montreal Neurological Institute (MNI) template using the DARTEL algorithm (Ashburner and Friston, 2005); (vi) The functional images were spatially normalized to the MNI-template by using the normalization parameters estimated by the DARTEL algorithm with voxels size set to 3 mm isotropic; (vii) Spatial smoothing was performed with a 6 mm full width at half maximum (FWHM) Gaussian kernel.

2.5. Spectral dynamic causal modeling

SpDCM uses a Bayesian model inversion procedure to infer from the measured cross-spectra density (CSD) of the BOLD signals on parameters of connections that link neural states in pre-defined networks of regions. The inverse Fourier transform of CSD corresponds to a cross-correlation

Table 1

Coordinates of the individual 5-mm³ sphere clusters of the left and right ROIs of the anterior and posterior insula, defined by Cauda et al. (2012) and Wright et al. (2016). K represents the number of voxels that are common between the insula ROIs and the insula masks from the Neuromorphometrics atlas provided by SPM12.

Seeds	Clusters	Left Hems.	MNI (x,y,z)	ROI(K)	Right Hems.	MNI (x,y,z)	ROI(K)
Ant. Ins.	1	-34.5	12.5	-2.5	34.5	12.5	-2.5
	2	-36.5	4.5	-3	38.5	5.5	-2.5
	3	-30.5	18.5	5.5	35.5	16.5	5.5
	4	-32.5	9	11.5	36.5	7	5
	5	-30.5	9	4.5	32.5	9	11.5
				59			62
Post. Ins.	1	-36.5	-7.5	-3.5	36.5	-4.5	-3
	2	-36.5	-10	4	38.5	-8	4
	3	-34.5	-13	10	34.5	-11	10.5
				24			25

function over time, which is the measure of the FC (Pearson’s correlation) at zero lag (Friston et al., 2014; Razi et al., 2015; Razi and Friston, 2016). In other words, inverting a probabilistic forward model (from hidden neural states to observed CSD of BOLD signals), spDCM estimates the directed connectivity among hidden neuronal states that best explains the measured FC between brain regions. A summary of spDCM can be found in supplementary material.

2.6. Region-of-interest time-series extraction

As regions of interest (ROI), we defined four ROIs located in the insula (two insula ROIs per hemisphere) and one within the hypothalamus (Fig. 2). For each insula ROI, we determined several coordinates (Table 1) to cover the functional differentiation within human insula (Wright et al., 2016). These coordinates were chosen based on FC studies that provided the association of the specific ROIs of the insula with other brain areas (Cauda et al., 2011) and which investigated the effect of hunger and satiety on the insular cortex (Wright et al., 2016). Subsequently, each coordinate was used to generate a 5 mm³ sphere cluster (Fig. 2A) by using the SPM Marsbar toolbox. Then, we summed up these clusters to create one combined seed for every subregion of the insula (i.e. anterior and posterior insula ROI). To avoid an overlap of the insula seed regions and other anatomical brain regions (i.e. regions outside the insula), we defined the final insula ROIs by finding common voxels between the insula ROIs and the corresponding insula masks from the Neuromorphometrics atlas provided by SPM12. The middle insula was not defined in order to avoid any overlap between the anterior and posterior insula ROIs.

The hypothalamus is notoriously difficult to examine in fMRI experiments as multiple factors can cause interference due to its anatomical position and small size (Dagher et al., 2017). Even though the hypothalamus has numerous subnuclei, we decided to focus our analysis on the whole hypothalamus as it would have been unrealistic to achieve

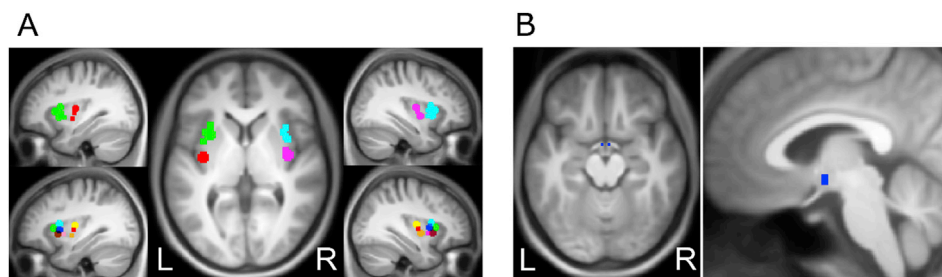


Fig. 2. Seeds superimposed on an average structural T1 image. (A) Middle picture and upper row: left and right anterior insula (green and cyan) and posterior insula (red and magenta) ROIs. Lower row: individual seeds in the right and left insula. (B) Hypothalamus (blue) ROI. L, left; R, right.

more spatially detailed results without running unique measurements adapted to the hypothalamus, which was not the primary goal of this study. The bilateral hypothalamus ROI (Fig. 2B) was based on the SPM Wake Forest University (WFU) Pickatlas toolbox (<http://www.fmri.wfubmc.edu/cms/software>, version 3.0; Maldjian et al., 2003).

The preprocessed rs-fMRI data for each subject per condition were entered into the general linear model (GLM) with a constant term, the confound regressors of the CSF signal and of the white matter signal and 24 head motion parameters (six standard realignment parameters, their derivative and the quadratic terms of these 12 realignment parameters; Friston et al., 1996), but not the average whole-brain signal. The applied temporal high pass filter of 1/100 Hz was included in the GLM model to remove slow frequency components caused by scanner drift. After estimation of the GLM model, we extracted time series from our ROIs, removing any signal that could be explained as a linear mixture of our 26 confound regressors. The time series was extracted using a singular value decomposition (SVD) procedure implemented in SPM12 and the first principal eigenvector was retained to represent the ROI time series (Fig. 3B). Fig. 3C and 3D shows the predicted cross-spectral density of the BOLD signals and the hidden neuronal states, respectively, of the winning model for a single subject. In four subjects, we were not able to calculate the time series of the bilateral hypothalamus ROI correctly because some of the voxels within the hypothalamus ROI belonged to the CSF (normalization artifact). Accordingly, these subjects were excluded from estimating spectral DCM parameters and the associated analyses. However, all 24 subjects were used for physiological and behavioral analyses as in our previous studies (Al-Zubaidi et al., 2018, 2019).

2.7. Spectral DCM and model space selection

The spDCM analyses were specified for each subject in each experimental condition (satiety-before, satiety-after, hunger-before and hunger-after oral glucose) separately using DCM12 (revision 7196) implemented in SPM12 (revision 7219). For each condition and participant, the average EC between the ROIs was modeled using different models. These different models varied in their directed connections between the five ROIs and were specified in order to explore alternative hypotheses of insula-hypothalamus network interactions. To avoid testing too many hypotheses and risk overfitting at the level of models (which, under flat priors on models, becomes more likely with the number of models compared), we tried to keep the model space as small as possible. For bilateral models, this is facilitated by the general anatomical principle that, with very few exceptions (like V1), reciprocal interhemispheric connections between homotopic areas in both hemispheres exist. This principle has been established in tract tracing studies in animals (e.g., see the early work in Macaques by McGuire et al., 1991) and human studies of brain connectivity (e.g., see the discussion and references in Stephan et al., 2007). The connections between hemispheres were supposed to take place either via hypothalamus, PINS and AINS (Fig. 4A: models 1–4) or via hypothalamic connections alone (Fig. 4A: models 5–8). Endocrine signaling of gut peptides that are related to promote meal initiation (e.g. ghrelin) or to promote meal cessation (e.g. insulin and leptin) reach specialized neurons within the hypothalamus and achieve their consequences by influencing brain regions involved in food intake regulation (Druce et al., 2004; Marić et al.,

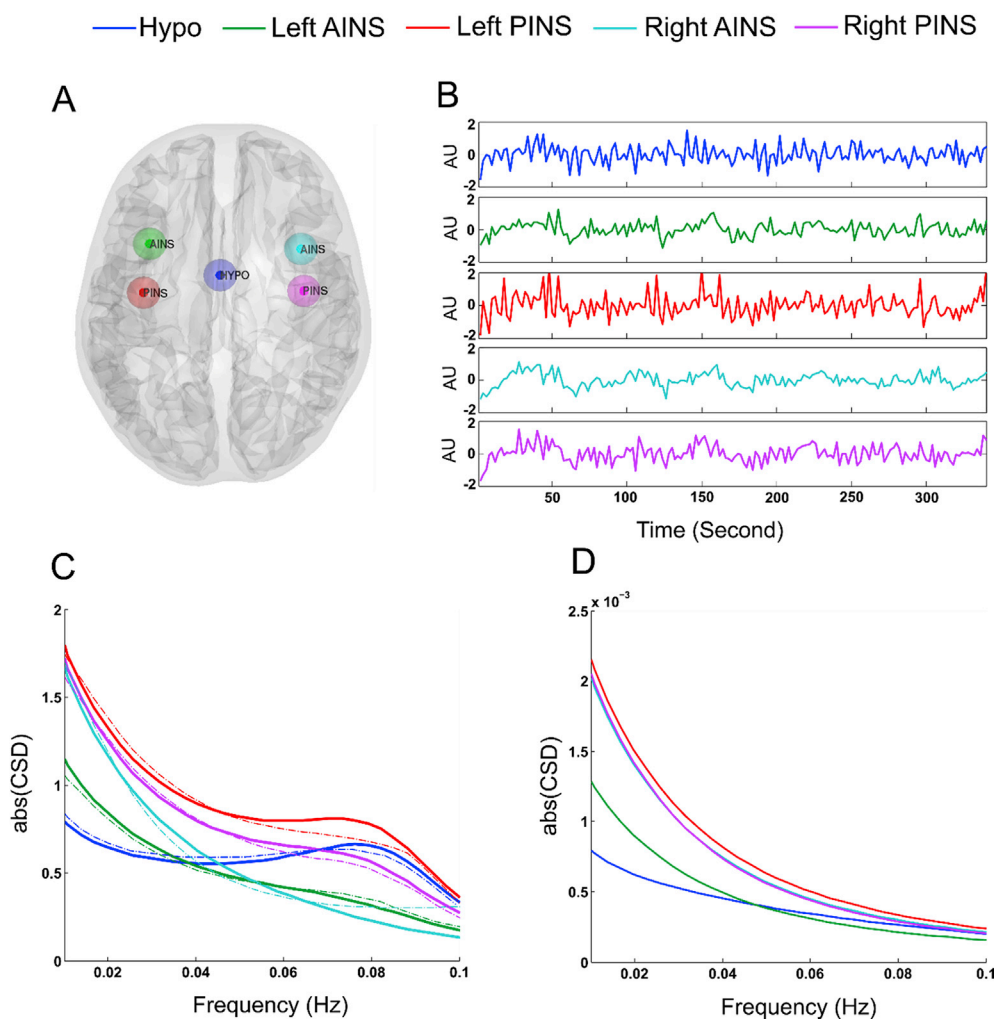


Fig. 3. Illustration of the hypothalamus-insula network and the results of the winning model for a single subject. The five spheres in (A) denote the five ROIs used in the spDCM analysis. The time series (B) from the five regions are the principle eigenvariate of the regions identified using a conventional SPM analysis. The observed (dashed lines) and predicted (solid lines) CSD of BOLD signals (C) by the winning model in the five ROIs. The underlying CSD predicted for the hidden neural states (D). Hypo = Hypothalamus; AINS = anterior Insula; PINS = posterior Insula; AU = arbitrary units; CSD = cross-spectral density; abs = absolute.

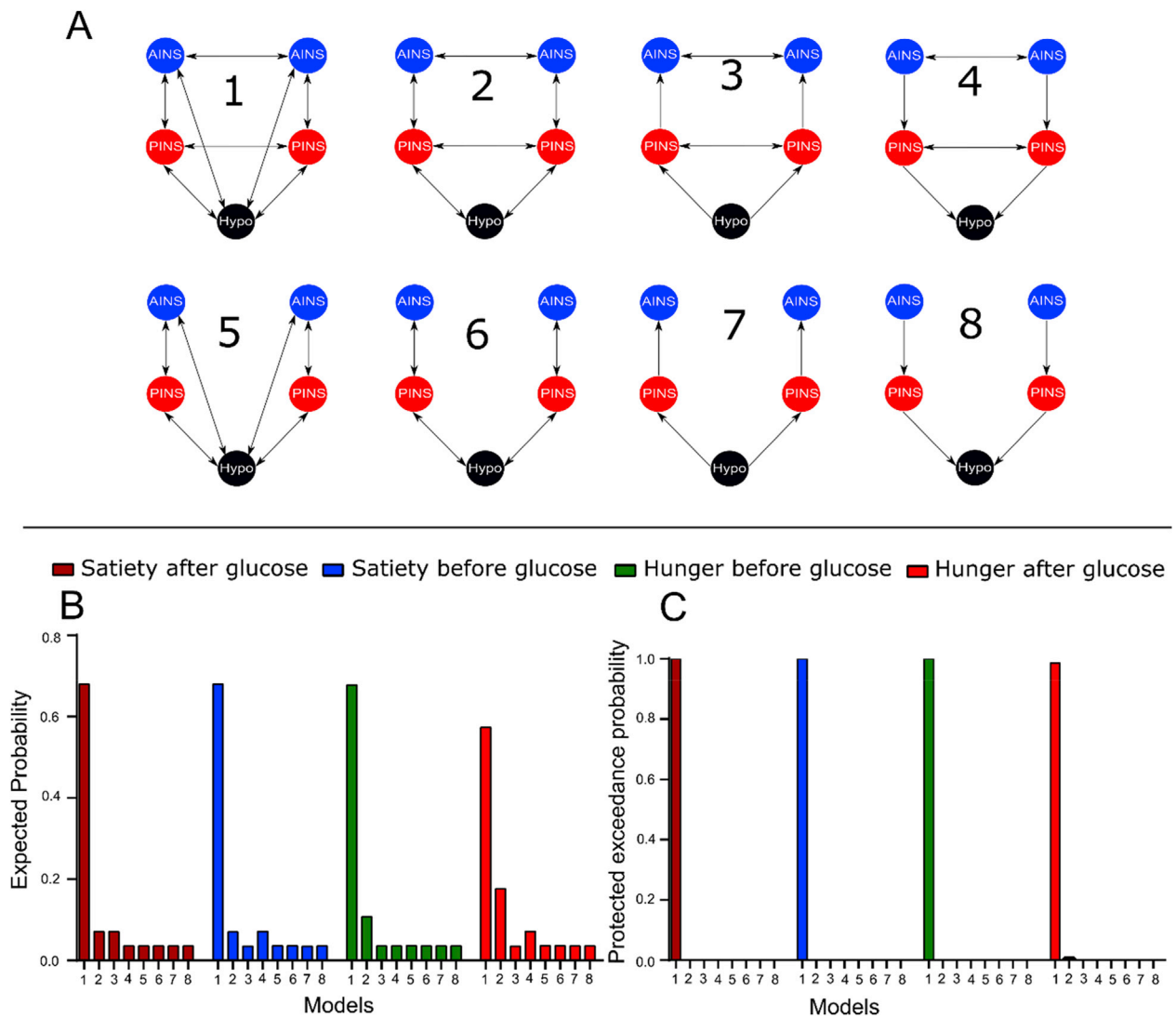


Fig. 4. Different plausible hypotheses and Bayesian model selection. (A) Possible connections among the five ROIs to explain the effective connectivity in the hypothalamus-insula network. Note that double arrow means reciprocal connections between two regions. (B) and (C) denote Bayesian model selection results per experimental condition for expected and protected exceedance probability in 8 models compared using RFX BMS, respectively. Hypo = Hypothalamus; AINS = anterior Insula; PINS = posterior Insula.

2014; Mayer, 2011; Zanchi et al., 2017). Furthermore, the hypothalamus is linked to brain regions, such as the insula and brainstem, which are involved in controlling the homeostatic energy balance (Barbas et al., 2003; Kullmann et al., 2014; Lemaire et al., 2011; Lips et al., 2014; Purnell et al., 2014; Wijngaarden et al., 2015). Therefore, we abstained from calculating models without any hypothalamic connections. The models in Fig. 4A display eight possible connections (parallel, i.e. models 1,2,5 and 6, forward, i.e. models 3 and 7, and backward, i.e. models 4 and 8) between the hypothalamus, PINS and AINS. After inverting and estimating the models, we used BMS to determine the most accurate model structure to describe the measured fMRI data (Stephan et al., 2009). The optimal model is determined by selecting the model with the best balance between data fitting (i.e. accuracy) and model complexity, as defined by the free energy bound on the model evidence (Penny et al., 2004). Random-effects BMS calculates the posterior model probability (that a specific model generated the data of a randomly chosen subject) and the protected exceedance probability (that a given model is more likely than any other model considered). Treating the model as a random variable in the population renders the method capable of dealing with population heterogeneity whilst being robust to outliers, or equivalent (Stephan et al., 2009).

To evaluate the success of model inversion or fit, the percent variance explained (or R^2) by the models for each experimental condition and subject were calculated using `spm_dcm_fmri_check.m.`, see Fig. S1; supplementary materials.

2.8. Parameter estimate of the winning model

The random-effects BMS procedures were used to determine the “winning model” for each prandial state condition (hunger or satiety) and glucose treatment (before or after glucose administration), separately. Then, we evaluated the endogenous connectivity parameters of the winning model in each condition using a second-level frequentist test. (Stephan et al., 2010). One-sample t-tests ($p < 0.05/16$, Bonferroni corrected for multiple comparisons) were applied to test whether the parameters of interest deviated significantly from zero. We reported the strength of the connections in Hz across participants (mean \pm SD) and the corresponding p -value.

The winning model of each condition resulted in the same model (see results section). Thus, we can examine the influence of conditions on the connections between ROIs. In the next step, the endogenous connectivity parameters of the winning model were submitted to rmANOVA with

factors prandial state (levels: hunger, satiety) and glucose administration (levels: before, and after treatment).

2.9. Associations between DCM parameters, physiological and behavioral responses

The rmANOVA on the NPEs (see Results section and Fig. 7), resulted in a significant main effect of the prandial state on the endogenous connection estimates from the right posterior to the right anterior insula (RPINS→RAINS) and from the right anterior to the right posterior insula (RPINS←RAINS). To investigate whether the changes in these connections were associated with physiological and behavioral responses, we used linear mixed-effects (LME) analysis which allows us to perform multiple regression while taking into account the repeated measures design of our subjects (Galecki and Burzykowski, 2013). The LME model identifies the linear relationships between a dependent variable (e.g. cortisol) and independent variables (e.g. NPEs), with coefficients that explain variation in respect to one or more grouping variables (e.g. experimental conditions). To this end, separate LME analyses were carried out for each of the four dependent variables (i.e. plasma cortisol, glucose and insulin levels as well as hunger ratings). Furthermore, only plasma cortisol, glucose and insulin levels narrowly associated with the rs-fMRI data collection were used as dependent variables (Fig. 1). For each of these four models, we entered the prandial state (levels: hunger vs. satiety) and glucose administration (levels: before vs. after glucose administration) as well as EC of RPINS→RAINS and RPINS←RAINS as a fixed effect with the intercepts for subjects as a random effect. As

post-hoc tests, a set of LME was used to analyze further the interaction effects. All continuous variables were Z-scored. LME analyses were performed using the lmer function in the lme4 package (Bates et al., 2015) for R (R Core Team, 2017) and sjPlot (Lüdtke, 2018). For significant slopes, we reported the regression coefficient parameter estimate (β).

In addition, we used multiple linear regression analysis to test for a statistically significant relationship between all connectivity estimates and participant's physiological (plasma cortisol, glucose and insulin levels) and behavioral (rating of hunger). For details, please see the supplementary material.

3. Results

3.1. Physiological and behavioral effects

Please note that the data on plasma glucose levels across both experimental days and behavioral response results have been published previously (Al-Zubaidi et al., 2018). This also applies to the average plasma glucose and insulin levels results of the second day of the experiment (Al-Zubaidi et al., 2019). In the present work, the average plasma levels of glucose, insulin and cortisol were calculated from the second day of the experiment for each subject under hunger and satiety conditions before and after glucose treatment (Fig. 1).

In order to familiarise the readers with the physiological and behavioral effects of our intervention and provide context for the new connectivity analyses, the following plasma glucous and insulin paragraphs re-describe our previously published results (Al-Zubaidi et al.,

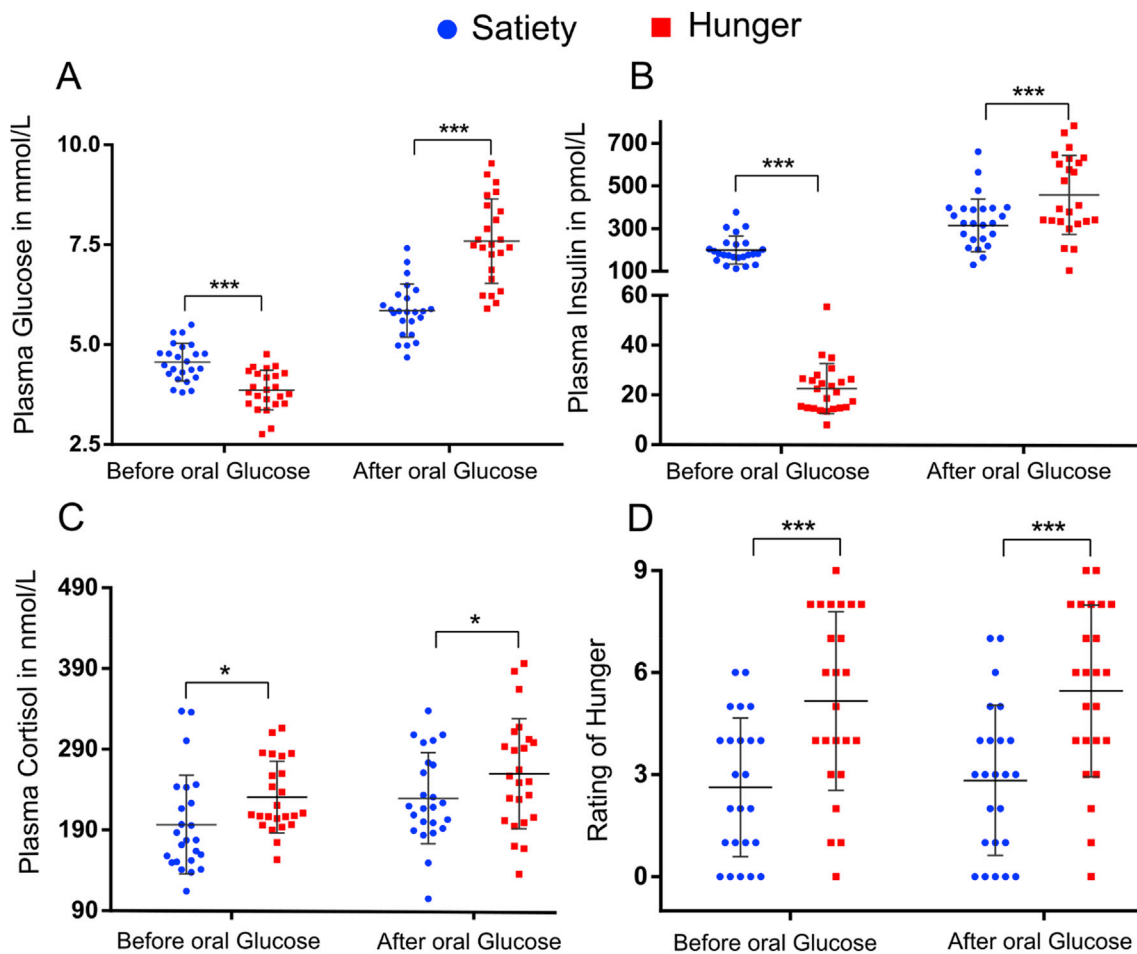


Fig. 5. Mean plasma glucose (A), plasma insulin (B), plasma cortisol levels (C) and hunger ratings (D) in the hunger and satiety conditions before and after the administration of glucose. * and *** represent the significant differences between conditions, at a threshold of $p < 0.01$ and $p < 0.0001$, respectively. Figures A, B and D are adapted from Al-Zubaidi et al. (2019). Figure D is adapted from Al-Zubaidi et al. (2018).

2019). The analysis of plasma glucose concentrations resulted in significant main effects of prandial state ($F_{(1,23)} = 23, p < 0.0001, \eta_p^2 = 0.50$) and glucose administration ($F_{(1,23)} = 256, p < 0.0001, \eta_p^2 = 0.92$) and a significant prandial state * glucose administration interaction ($F_{(1,23)} = 53, p < 0.0001, \eta_p^2 = 0.70$; see Fig. 5A). Post hoc t-tests performed to reveal the interaction driving effects indicated that the glucose level before the glucose administration was significantly ($T_{(23)} = 4.5, p < 0.0001$) higher in the satiated ($M = 4.6$ mmol/L, $SD = 0.5, 95\% CI[4.4, 4.8]$) compared to the hunger state ($M = 3.9$ mmol/L, $SD = 0.5, 95\% CI[3.7,4.1]$). After glucose administration, this effect reversed and a significantly ($T_{(23)} = 7.4, p < 0.0001$) higher glucose level was seen in the hungry ($M = 7.6$ mmol/L, $SD = 1.1, 95\% CI[7.2,8.1]$) compared to the satiated state ($M = 5.9$ mmol/L, $SD = 0.7, 95\% CI[5.6,6.1]$). This effect indicates reduced responsiveness to the circulating glucose during the satiated state. For the pre-glucose administration (Fig. 1C, left y-axis) hypoglycemia is defined as blood glucose levels below 3.9 mmol/L, euglycemia as fasting glucose levels between 3.9 and 5.6 mmol/L, and hyperglycemia as fasting glucose levels greater than 6.9 mmol/L. For the post-glucose administration (Fig. 1C, right y-axis, at 120 min after glucose administration), hypoglycemia is defined as glucose levels below 3.9 mmol/L, euglycemia is considered as glucose levels between 3.9 and 7.8 mmol/L, and hyperglycemia as glucose levels equal or greater than 11.1 mmol/L (all thresholds are according to the American Diabetes Association, 2020).

The analysis of plasma insulin (Fig. 5B) concentrations revealed a significant main effect of glucose administration ($F_{(1,23)} = 106, p < 0.0001, \eta_p^2 = 0.82$) and a significant prandial state * glucose administration interaction ($F_{(1,23)} = 102, p < 0.0001, \eta_p^2 = 0.81$), but no significant main effect of the prandial state ($F_{(1,23)} = 0.65, p = 0.4, \eta_p^2 = 0.03$). The post hoc analysis showed significantly ($T_{(23)} = 13.5, p < 0.0001$) higher insulin concentrations in the satiated state ($M = 198.8$ pmol/L, $SD = 65.2, 95\% CI[171.3226.3]$) compared to the hunger state ($M = 22.5$ pmol/L, $SD = 10.1, 95\% CI[18.3,26.8]$) before the administration of glucose. After glucose administration, this effect reversed and significantly ($T_{(23)} = 4.2, p < 0.0001$) higher insulin concentrations were observed in the hunger state ($M = 457.9$ pmol/L, $SD = 185.6, 95\% CI[379.6536.3]$) than in the satiated state ($M = 314.6$ pmol/L, $SD = 123.5, 95\% CI[262.5366.9]$) indicating reduced responsiveness to circulating insulin. Due to the fasting-induced insulin resistance, the body secretes more insulin to overcome this resistance.

Furthermore, for plasma cortisol (see Fig. 5C) significant main effects of prandial state ($F_{(1,23)} = 9.1, p = 0.006, \eta_p^2 = 0.28$) and glucose administration ($F_{(1,23)} = 7, p = 0.01, \eta_p^2 = 0.24$) were revealed with no significant interaction ($F_{(1,23)} = 0.03, p = 0.9, \eta_p^2 = 0.001$). Before glucose treatment, the plasma cortisol level for the hunger state ($M = 230$ nmol/L, $SD = 44.4, 95\% CI[205.5253.1]$) was higher ($T_{(23)} = 2.1, p = 0.4$) compared to the satiated state ($M = 196.6$ nmol/L, $SD = 61.2, 95\% CI[170.8222.4]$). A similar effect was found after glucose treatment, the plasma cortisol level was greater ($T_{(23)} = 2.2, p = 0.4$) in the hunger ($M = 260$ nmol/L, $SD = 68.3, 95\% CI[230.8288.5]$) compared to a satiated state ($M = 230$ nmol/L, $SD = 56.4, 95\% CI[211.9249.4]$). Our data thus do not provide evidence for a significant impact of glucose treatment on how the prandial states affected the plasma cortisol levels.

Finally, we also re-describe our previous published behavioral effects (Al-Zubaidi et al., 2018, 2019). Concerning subjective hunger ratings (Fig. 5D) a significant main effect of prandial state ($F_{(1,23)} = 28.9, p < 0.001, \eta_p^2 = 0.56$) with higher hunger ratings in the hunger state ($M = 5.2, SD = 2.6, 95\% CI[4.3,6.3]$) compared to the satiated state ($M = 2.6, SD = 2.1, 95\% CI[2.1,3.4]$) was obtained but neither the main effect of glucose administration ($F_{(1,23)} = 0.34, p = 0.6, \eta_p^2 = 0.02$) or a prandial state * glucose administration interaction ($F_{(1,23)} = 0.02, p = 0.9, \eta_p^2 = 0.001$). These findings confirm the success of our fasting treatment.

3.2. Bayesian model selection

When testing for the model structure that explains the rs-fMRI data best by using RFX BMS, model 1 (Fig. 4B) had the highest protected exceedance probability (PXP = 0.99) at the group level for each experimental condition (shown in Fig. 4C). The lower evidence of models without interhemispheric connections (models 5–8) indicates that lack of inter-hemispheric connectivity led to a worse explanation of the participants' network activity. This result suggests that the reciprocal connections, both within hemispheres (i.e. hypothalamus-PINS-AINS) and between hemispheres were necessary network features.

3.3. Model parameters

We investigated whether the EC among the ROIs estimated using the winning model were significantly non-zero separately for each condition. In Table 2 and Fig. 6 we show the mean connection strength (in Hz) and the results from the one-sample t-tests. For simplicity, self-connections are not included in the table and graph. To sum up, in the satiety condition after oral glucose intake we found that the connection strength from left anterior insula (LAINS) to left posterior insula (LPINS) was significantly different from zero ($M = 0.5, SD = 0.48, T_{(19)} = 4.7, 95\% CI[0.28,0.73], p = 0.0002$, surviving Bonferroni correction of $p < 0.5/16$). Furthermore, in the hunger condition before oral glucose intake we found that the connection from the right posterior insula (RPINS) to the right anterior insula (RAINS) was also significantly different from zero ($M = 0.41, SD = 0.46, T_{(19)} = 4, 95\% CI[0.2,0.4], p = 0.001$, surviving Bonferroni correction of $p < 0.5/16$), too. Finally, we did not find any significant connections from or to the hypothalamus.

A two-way rmANOVA was conducted to determine the influence of two independent variables (prandial state and glucose administration) on endogenous connection estimates of the winning model. Both prandial state (hunger and satiety) and administration (before and after glucose intake) consisted of two levels. There were no significant effects of glucose administration and interactions between both factors on all endogenous connection estimates. We found a significant ($p < 0.05$) main effect of prandial state on the endogenous connections from RPINS to RAINS (forward connection, RPINS→RAINS) ($F_{(1,19)} = 8.8, p = 0.008, \eta_p^2 = 0.32$), indicating significant stronger connectivity during hunger ($M = 0.37$ Hz, $SD = 0.49, 95\% CI[0.2,0.6]$) compared to satiety ($M = 0.15$ Hz, $SD = 0.54, 95\% CI[-0.04,0.32]$). Also, we observed a significant main effect of prandial state on the endogenous connections from RAINS to RPINS (backward connection, RPINS←RAINS) ($F_{(1,19)} = 4.7, p = 0.04, \eta_p^2 = 0.2$) indicating that the satiated state ($M = 0.12$ Hz, $SD = 0.49, 95\% CI[-0.05,0.29]$) showed higher connectivity strength compared to the hunger state ($M = -0.11$ Hz, $SD = 0.55, 95\% CI[-0.3,0.09]$), as shown in Fig. 7.

3.4. Associations between DCM parameters, physiological and behavioral responses

LME analyses revealed significant interactions ($\beta = -0.8, 95\% CI[-1.4, -0.24], F_{(1,64)} = 7.7, p = 0.007$) between RPINS→RAINS connection (forward connection) strength, prandial state and glucose administration in explaining cortisol levels (Fig. 8A). To further analyze the interaction-driving factor, we performed LME analyses per glucose treatment condition separately, as post-hoc tests. We found that the interactions between RPINS→RAINS and prandial state predicting the cortisol levels was significant ($\beta = 0.9, 95\% CI[0.26,1.6], p = 0.01$) before, but not ($\beta = -0.5, 95\% CI[-1.4,0.3], p = 0.2$) after oral glucose. More precisely, before oral glucose treatment, the forward RPINS→RAINS connectivity showed a strong positive ($\beta = 0.7, 95\% CI[0.1,1.3], p = 0.03$) and negative ($\beta = -0.5, 95\% CI[-0.92,-0.02], p = 0.06$) relation to cortisol levels in hunger and satiety conditions, respectively. Whereas, after oral glucose treatment, the relationship between RPINS→RAINS strength and cortisol

Table 2

Posterior estimates of effective connectivity (Hz) in the winning model (mean ± SD) per experimental condition. Using one-sample t-tests, we tested whether the effective connectivity was significantly different from zero.

Connections			Satiety				Hunger			
			Before Glucose		After Glucose		Before Glucose		After Glucose	
			Strength (Hz)	P-Value	Strength (Hz)	P-Value	Strength (Hz)	P-Value	Strength (Hz)	P-Value
LAINS	→	Hypo	-0.07 ± 0.61	0.8	-0.08 ± 0.37	0.15	0.04 ± 0.68	0.35	-0.01 ± 0.44	0.21
LPINS	→	Hypo	-0.06 ± 0.29	0.9	-0.04 ± 0.28	0.85	-0.12 ± 0.41	0.85	-0.01 ± 0.23	0.5
RAINS	→	Hypo	-0.02 ± 0.72	0.32	0.09 ± 0.64	0.85	-0.11 ± 0.51	0.07	0.09 ± 0.51	0.92
RPINS	→	Hypo	0.07 ± 0.56	0.46	-0.04 ± 0.38	0.95	0.1 ± 0.44	0.91	-0.11 ± 0.42	0.26
Hypo	→	LAINS	0.03 ± 0.61	0.62	0.17 ± 0.51	0.34	0.13 ± 0.62	0.77	0.18 ± 0.61	0.89
LPINS	→	LAINS	0.09 ± 0.43	0.16	0.15 ± 0.53	0.46	0.26 ± 0.35	0.03	0.2 ± 0.39	0.04
RAINS	→	LAINS	0.24 ± 0.59	0.16	0.31 ± 0.51	0.008*	0.06 ± 0.85	0.21	0.23 ± 0.73	0.11
Hypo	→	LPINS	-0.02 ± 0.68	0.37	0.03 ± 0.67	0.57	-0.01 ± 0.68	0.2	0.13 ± 0.83	0.87
LAINS	→	LPINS	0.29 ± 0.89	0.35	0.5 ± 0.48	0.0002#	0.12 ± 0.72	0.07	0.15 ± 0.63	0.06
RPINS	→	LPINS	0.25 ± 0.73	0.12	0.003 ± 0.72	0.43	0.42 ± 0.75	0.006*	0.22 ± 0.58	0.05
Hypo	→	RAINS	-0.09 ± 0.38	0.91	-0.07 ± 0.45	0.55	0.13 ± 0.32	0.36	0.01 ± 0.38	0.43
LAINS	→	RAINS	0.16 ± 0.47	0.08	0.19 ± 0.39	0.009*	0.16 ± 0.55	0.78	0.14 ± 0.37	0.17
RPINS	→	RAINS	0.16 ± 0.56	0.11	0.13 ± 0.52	0.67	0.41 ± 0.46	0.001#	0.32 ± 0.53	0.004*
Hypo	→	RPINS	-0.07 ± 0.43	0.58	-0.01 ± 0.59	0.65	-0.01 ± 0.47	0.33	0.12 ± 0.47	0.24
LPINS	→	RPINS	0.11 ± 0.35	0.14	0.25 ± 0.36	0.006*	0.1 ± 0.54	0.11	0.21 ± 0.42	0.02
RAINS	→	RPINS	0.19 ± 0.52	0.23	0.05 ± 0.46	0.29	-0.14 ± 0.59	0.72	-0.08 ± 0.52	0.82

The significant ($p < 0.05$) connections are shown in bold. The * and # represent significance at $p < 0.01$ and after Bonferroni correction ($p < 0.05$), respectively. Abbreviations: LAINS, left anterior insula; LPINS, left posterior insula; Hypo, hypothalamus; RAINS, right anterior insula; RPINS, right posterior insula.

disappeared for both the hunger ($\beta = -0.4$, 95% CI[-0.98,0.02], $p = 0.08$) and satiety ($\beta = -0.03$, 95% CI[-0.62,0.7], $p = 0.9$) conditions.

Finally, the interactions between the RPINS←RAINS connection strength (backward connection) and prandial state significantly predicted cortisol levels (Fig. 8B; $\beta = -0.7$, 95% CI[-1.3,-0.13], $F_{(1,64)} = 5.7$, $p = 0.02$) and the hunger ratings (Fig. 8C; $\beta = -0.6$, 95% CI[-1.2,-0.08], $F_{(1,64)} = 5$, $p = 0.03$). More precisely, the backward RPINS ←RAINS connection strength showed a positive relations to both, the cortisol levels ($\beta = 0.5$, 95% CI[-0.1,1.1], $p = 0.1$) and hunger ratings ($\beta = 0.7$, 95% CI[0.24,1.1], $p = 0.007$) in the satiety condition. In contrast, in the hunger condition, the RPINS←RAINS connection strength was negatively

and non-significantly associated with cortisol levels ($\beta = -0.3$, 95% CI [-0.65,0.1], $p = 0.2$) and hunger ratings ($\beta = -0.5$, 95% CI[-1.1,0.02], $p = 0.08$). In addition, we observed no significant relations between the glucose or insulin levels and the forward RPINS→RAINS or backward RPINS←RAINS connection strengths.

Using multiple linear regression, only blood cortisol levels before glucose administration were significantly associated with connectivity estimates (Fig. S3, supplementary material).

4. Discussion

The purpose of this study was to investigate the influence of prandial state (hunger vs. satiety) and glucose administration on the pattern of EC between hypothalamus, PINS and AINS as core components of networks supporting both ingestive behavior and interoception. Applying spDCM to rs-fMRI data, we estimated directed connection strengths between brain regions of interest at neuronal states. Our results suggest that effective connection strengths were modulated by changes in prandial states, but not glucose administration. Specifically, during the hunger condition, the forward connection strength from right PINS to right AINS was increased, while during satiety, the backward connection strength from right AINS to right PINS was increased (Fig. 7). These findings (in particular the increase of forward connections during hunger) are compatible with predictions of recent computational theories that view interoception as a hierarchical Bayesian inference process and predict differences in insular connectivity patterns between dyshomeostatic and homeostatic states, such as hunger versus satiety (Stephan et al., 2016). Furthermore, we found significant statistical associations between insular connectivity on the one hand and cortisol levels and hunger ratings on the other hand. Our findings are relevant to contemporary research on interoception and ingestive behavior as they demonstrate changes in brain connectivity that are consistent with theories of interoception and illustrate that network properties are linked to both physiological (endocrine) states and subjective experience.

4.1. Changes in physiological and behavioral responses related to metabolic conditions

As previously reported (Al-Zubaidi et al., 2018), stronger feelings of hunger in the hunger condition show that the experimental manipulation was successful (Fig. 5D).

Moreover, we found the typical constellation of fasting-induced

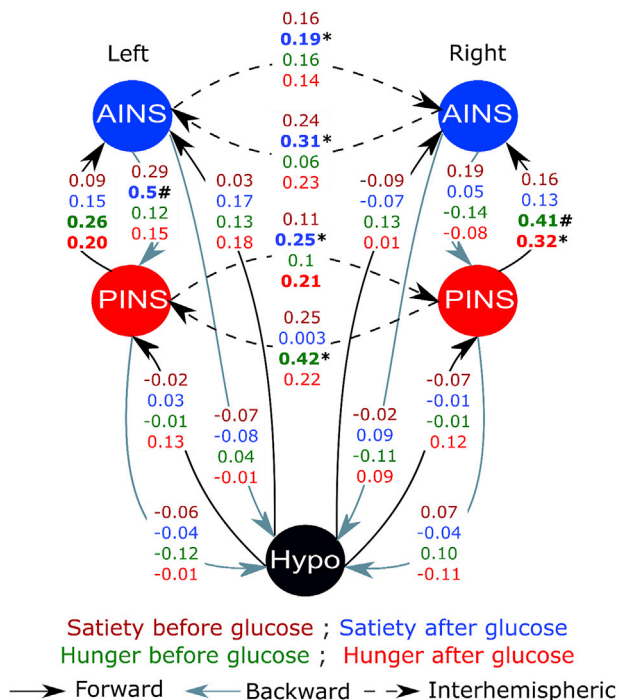


Fig. 6. The winning model at the group level and its mean connectivity parameters (in Hz) per experimental condition. The significant ($p < 0.05$) connections are shown in bold. The * and # represent significance at $p < 0.01$ and after Bonferroni correction ($p < 0.05$), respectively.

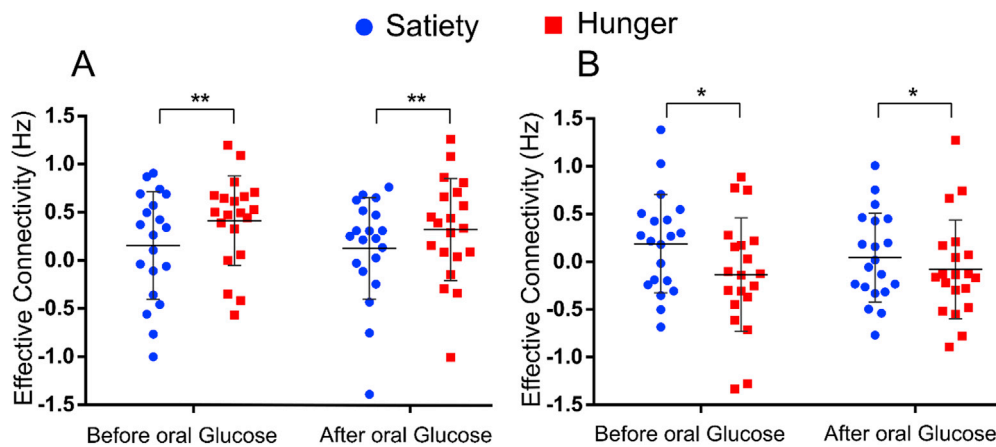


Fig. 7. Effective connectivity parameters that showed a significant main effect of the metabolic state (hunger vs. satiety). (A) Strength of the forward connections from RPINS to RAINS (RPINS→RAINS). (B) Strength of the backward connections from RAINS to RPINS (RPINS←RAINS). * and ** represent the significant differences between conditions, $p < 0.05$ and $p < 0.01$, respectively.

insulin resistance, reflected in increased glucose concentrations after glucose administration in the hunger condition (Anderson and Matsa, 2011; Clayton et al., 2016; Frank et al., 2013; Schweinhardt et al., 2006). In contrast, before glucose administration, the concentrations of plasma glucose and insulin levels were higher in the satiety condition compared to the hunger condition (Fig. 1B, C, 5A and 5B).

Finally, blood cortisol concentrations increased as expected during the fasting relative to the satiety condition (Fig. 5C). Previous studies have shown a direct relationship between increases in cortisol levels and dieting or starvation due to changes in biological functioning such as freeing of energy and psychological influences like resisting food temptation (Johnstone et al., 2004; Tomiyama et al., 2010).

To conclude, our study shows differential effects in response to glucose ingestion of three investigated physiological markers, glucose, insulin and cortisol, during different prandial states, namely hunger and satiation, in healthy normal-weight males.

4.2. Changes in endogenous connectivity related to metabolic conditions

Spectral DCM analysis is a framework to model the EC between ROIs based on the FC in rs-fMRI data as well as make inferences about specific parameter changes (Friston et al., 2014). BMS reveals the most likely model (i.e. possible way of connections) among a set of different models to explain the data by taking into account the balance between complexity and goodness-of-fit (Penny et al., 2004; Pitt and Myung, 2002; Stephan and Friston, 2010). In this work, BMS suggested that the fully connected model (model 1 in Fig. 4A) was the best model in all experimental conditions (Fig. 4C).

After fasting, we observed a strong positive connection ($+0.36 \pm 0.05$) in the right hemisphere from PINS to AINS (RPINS→RAINS; Figs. 6 and 7A) which suggests a more intense influence of interoceptive inputs represented in PINS on AINS function (Chang et al., 2013; Kann et al., 2016; Penfield and Faulk, 1955; Wang et al., 2008). In the same condition, a negative connection (-0.11 ± 0.03) from right AINS to right PINS (RPINS←RAINS; Figs. 6 and 7B) indicated an inhibitory influence of the anterior insula on posterior insula during hunger. These findings can be interpreted in the context of recent theories of interoception that we describe below.

Craig (2009) suggested a pathway that maps objective representations of body conditions onto a subjective representation of the physical self, via posterior-to-anterior pathways within the right insula. Our results demonstrate that the connection strength from the right PINS to the right AINS is increased in hunger relative to satiety. This finding

indicates that the connectivity within the right posterior-to-anterior insula pathway (RPINS→RAINS) can be altered by food intake because those changes were only observed in response to changes in prandial states, but not in glucose treatment. Our observations allow for the speculative interpretation that changes within this pathway, which we also found to be related to cortisol levels, could reflect the perceived salience of internal bodily states (Craig, 2014; Kann et al., 2016). In contrast, we observed a decreased strength of the backward connection from right AINS to right PINS (RPINS←RAINS) during hunger compared to satiety conditions. One could assume that the reduced strength of EC from RAINS to RPINS might be the result of bodily signals forwarded from posterior to anterior insula (RPINS→RAINS), which may become more salient in the hunger condition. An alternative (and equally tentative) interpretation refers to recent theories that PINS, AINS and ACC are part of a hierarchical system for interoception, i.e. inference on bodily (metabolic, immunological, physical) states and homeostatic/allostatic regulation (Seth et al., 2012; Stephan et al., 2016). More specifically, these theories view interoception as a “predictive coding” (Friston, 2005; Rao and Ballard, 1999) process during which predictions are transmitted via backward connections and prediction errors via forward connections. Predictions concern expected bodily states, e.g. within the typical homeostatic range, or represent forecast bodily consequences of particular actions or environmental dynamics. The latter can be used to adjust homeostatic setpoints in an anticipatory actions and thus mediate prospective (allostatic) control (Stephan et al., 2016). By contrast, (interoceptive) prediction errors signal the mismatch between the actual and predicted bodily states. Interoceptive prediction errors thus signal that bodily states deviate from what is expected and serve as a driving force behind homeostatic regulation (Pezzulo et al., 2015). Thus, the strengthening of forwarding connections from PINS to AINS during hunger states could be potentially interpreted as the reflection of tonically increased prediction error signals, while the negative (inhibitory) backward connections could reflect the effect of predictions (which, in predictive coding, are subtracted from actual states).

4.3. Associations between DCM parameters, physiological and behavioral responses

The relationship between the strength of RPINS→RAINS connection (i.e. forward connection) and plasma cortisol levels was modulated by prandial states before oral glucose intake (Fig. 8A). However, the modulation of the association between the strength of RPINS←RAINS connection (i.e. backward connection) and both plasma cortisol levels

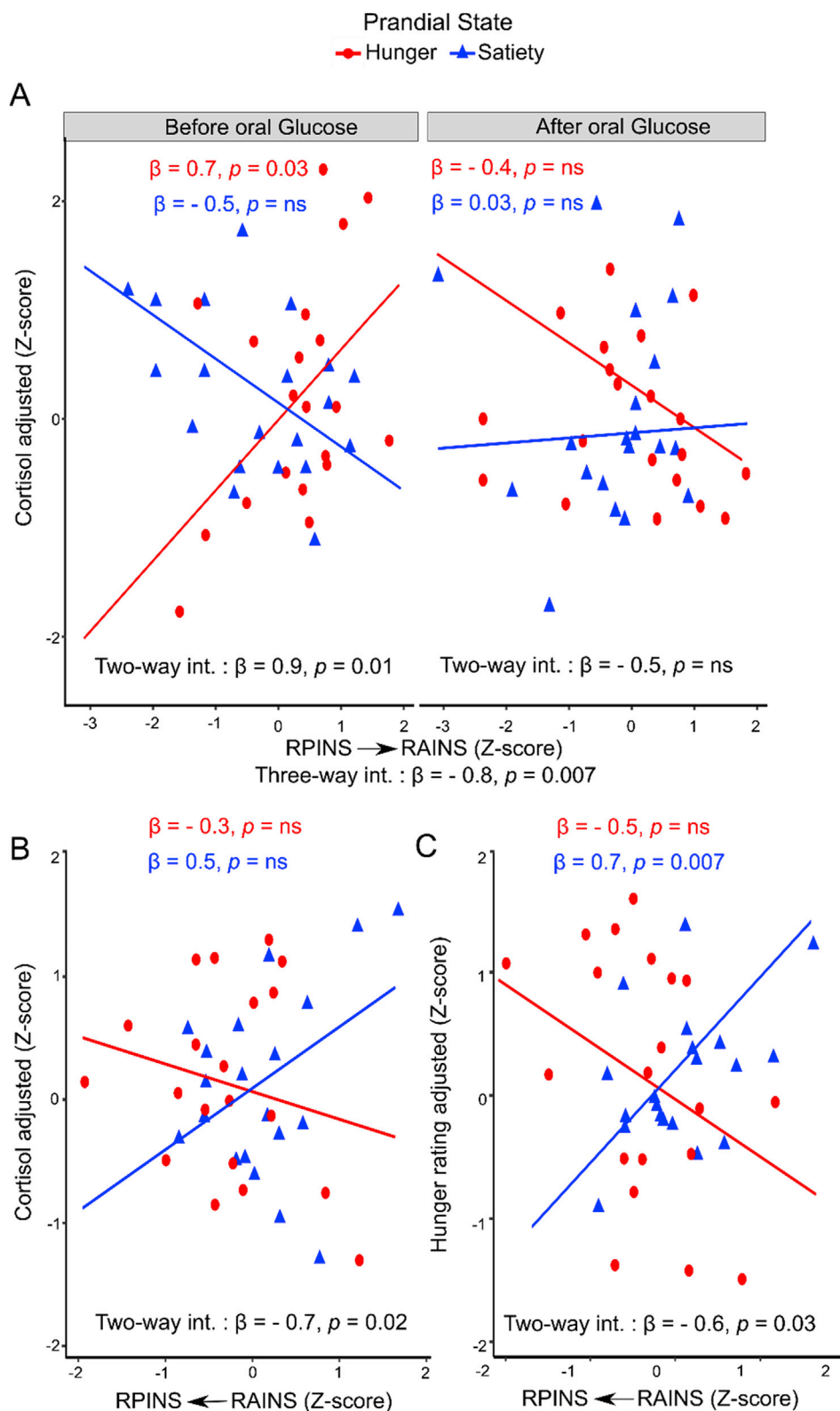


Fig. 8. Interactions between covariates in the linear mixed effects model predicting individual physiological and behavioral responses. (A) Interaction of RPINS→RAINS connectivity (forward connection) with the prandial state (levels: hunger vs. satiety) and glucose administration (levels: before vs. after glucose administration). (B) and (C) interaction of RAINS←RPINS connectivity (backward connection) with prandial state predicting cortisol levels and hunger ratings, respectively. Solid lines indicate linear regression fit between the dependent variables (y-axis) and covariates (x-axis). int.: interaction. RAINS: right anterior insula. RPINS: right posterior insula. β : slope coefficient parameter estimate resulting from linear mixed-effects models. ns: represent no significance.

and hunger ratings depended only on the prandial states and were therefore independent of glucose treatment (Fig. 8B and C, respectively). Our findings suggest that glucose administration affected the relationship between cortisol and forward connectivity estimates. However, no such modulation was found for the relationship between cortisol and the backward connection estimates.

4.4. Limitations

Our study design and analyses have several noteworthy limitations. First, there was no significant effect of hunger on connections from the hypothalamus to AINS or PINS and vice versa. It has been shown that nuclei of the hypothalamus stimulate feeding (lateral hypothalamus, LH)

or inhibit feeding behavior (ventromedial hypothalamus nucleus, VMN) (Mayer and Thomas, 1967; Suzuki et al., 2010). This dual function of hypothalamic nuclei, as well as their small size, might have led to a canceling of the two opposing signals (De Silva et al., 2012). Moreover, the acquisition parameters of the fMRI were not optimized to differentiate between different nuclei in such a small subcortical structure. Additionally, the hypothalamic regions are located in close vicinity to the air-tissue boundaries of surrounding sinuses and thus extracted BOLD signals from such regions are susceptible to loss (Ojemann et al., 1997). In the present study, we did not conduct any quality control procedures that were specific for the hypothalamus.

Second, due to the rather small sample size, we could not directly investigate the relation between all NPEs (i.e. connections) and hormone variables (i.e. plasma glucose, insulin and cortisol levels) using standard multiple linear regression and used principal components as regressors instead. To establish a direct relationship between NPEs and hormonal data, a replication of the current study with a larger sample would be desirable.

Third, to limit the influence of the hormonal cycle, we only included healthy lean young men in the current study, which therefore may not be generalizable to other populations. Functional neuroimaging studies have shown differences in response to food taste (e.g. sweet, liquid meals) and even to odours of sweet (e.g. chocolate cake) under hunger and satiety conditions in several sexually dimorphic and BMI-sensitive brain regions (Bragulat et al., 2010; Carnell et al., 2012; DelParigi et al., 2005; Haase et al., 2011). Future studies could address this question by also including female and overweight participants and thus discuss the relationship between spDCM results and sex or BMI.

Fourth, the finding that subjects showed enhanced cortisol levels in the hunger condition suggests that subjects might have been more vigilant in this condition. Future studies should actively control for alertness (with e.g. eye-tracking) in order to rule out this confound.

Finally, as mentioned in the introduction, the hypothalamus and insular cortex are involved in a variety of functions related to interoception and homeostatic regulation in response to different metabolic states. Here, we investigated a particular set of models comprising five brain regions to address specific questions about relationships among connectivity in this network and physiological states. It is important to keep in mind that the models we examined are (necessarily) wrong in that they are enormously simplified compared to the real neural system and only consider a small number of potentially relevant regions. Including additional regions and connections (e.g., hypothalamic sub-nuclei) could change the input structure to (some or all) regions and may alter the results. This “missing region” problem – and other caveats of effective connectivity analyses with DCM (and other methods) – are well known and have been discussed previously (e.g., Daunizeau et al., 2011). It is therefore important to establish the “utility” of the particular model we identified, for example, whether the inferred connection strengths relate to independent variables (e.g., physiological states) and whether these connectivity estimates allow for out-of-sample predictions. While the former has been examined in this study, the latter will need to be investigated in future work.

5. Conclusions

Hypothalamic and insular cortex activation has previously been found to reflect changes in the homeostatic energy balance. By applying spDCM and BMS analyses to rs-fMRI data, we examined whether the prandial state (hunger vs. satiety) and glucose administration (before vs. after) would modulate the EC between brain regions involved in ingestive behavior. Our most plausible model in all prandial and glucose conditions comprised intra- and interhemispheric connections within a bilateral hypothalamus-PINS-AINS network model. EC was significantly increased for the forward connection RPINS→RAINS but decreased for the backward connection RPINS←RAINS under hunger compared to satiety, with no influence of glucose treatment. Furthermore, the strength

of RPINS→RAINS connectivity was positively associated with plasma cortisol levels in the hunger condition, particularly before glucose administration. Overall, these results illustrate how connections among brain regions involved in interoception and homeostatic regulation change between hunger and satiety and provide a basis for future investigations of hypothalamic-insular networks in the context of food intake.

Author's contribution

AA managed the literature searches, wrote the first draft of the manuscript and performed data analysis. KJC and TFM designed the study. AA, MH, and JMN participated in the data collection. AA, SI and KES designed the statistical analysis. SI, KSE, MBR, HK, AM and TFM contributed with the interpretation of the results. All authors contributed to the manuscript and approved its final version.

Declaration of competing interest

The authors do not report any conflict of interest.

CRediT authorship contribution statement

Arkan Al-Zubaidi: Investigation, Formal analysis, Writing - original draft. **Sandra Iglesias:** Formal analysis, Writing - review & editing. **Klaas E. Stephan:** Methodology, Formal analysis, Writing - review & editing. **Macià Buades-Rotger:** Methodology, Formal analysis, Writing - review & editing. **Marcus Heldmann:** Data curation, Investigation, Project administration, Validation. **Janis Marc Nolde:** Investigation, Writing - review & editing. **Henriette Kirchner:** Methodology, Writing - review & editing. **Alfred Mertins:** Methodology, Writing - review & editing. **Kamila Jauch-Chara:** Conceptualization, Supervision, Funding acquisition. **Thomas F. Münte:** Conceptualization, Supervision, Funding acquisition, Writing - review & editing.

Acknowledgments

This work was supported by a grant of the German Research Foundation to the Research Training Group 1957 ‘Adipocyte-Brain Crosstalk’ and the SFB TR 134, project C1 to TFM.

KES acknowledges generous support by the René and Susanne Braginsky Foundation and the University of Zurich. AA thanks Prof. Jonas Obleser and Dr. Sarah Tune for helpful comments regarding the linear mixed-effects analysis. AA and JMN thank Dr. Sophia G Connor for her helpful comments and editorial support.

Appendix A. Supplementary data

Supplementary data to this article can be found online at <https://doi.org/10.1016/j.neuroimage.2020.116931>.

References

- Al-Zubaidi, A., Heldmann, M., Mertins, A., Brabant, G., Nolde, J.M., Jauch-Chara, K., Münte, T.F., 2019. Impact of hunger, satiety, and oral glucose on the association between insulin and resting-state human brain activity. *Front. Hum. Neurosci.* 13, 162. <https://doi.org/10.3389/fnhum.2019.00162>.
- Al-Zubaidi, A., Heldmann, M., Mertins, A., Jauch-Chara, K., Münte, T.F., 2018. Influences of hunger, satiety and oral glucose on functional brain connectivity: a multimethod resting-state fMRI study. *Neuroscience* 382, 80–92. <https://doi.org/10.1016/j.neuroscience.2018.04.029>.
- Anderson, M.L., Matsa, D.A., 2011. Are restaurants really supersizing America? *Am. Econ. J. Appl. Econ.* 3, 152–188. <https://doi.org/10.1257/app.3.1.152>.
- Ashburner, J., Friston, K.J., 2005. Unified segmentation. *Neuroimage* 26, 839–851. <https://doi.org/10.1016/j.neuroimage.2005.02.018>.
- Barbas, H., Saha, S., Rempel-Clower, N., Ghashghaei, T., 2003. Serial pathways from primate prefrontal cortex to autonomic areas may influence emotional expression. *BMC Neurosci.* 4, 1–12. <https://doi.org/10.1186/1471-2202-4-25>.
- Bates, D.M., Maechler, M., Bolker, B., Walker, S., 2015. lme4: linear mixed-effects models using Eigen and S4 classes. *J. Stat. Software*.

- Begg, D.P., Woods, S.C., 2013. The endocrinology of food intake. *Nat. Rev. Endocrinol.* 9, 584. <https://doi.org/10.1038/nrendo.2013.136>.
- Bragulat, V., Dzemidzic, M., Bruno, C., Cox, C.A., Talavage, T., Considine, R.V., Kareken, D.A., 2010. Food-related odor probes of brain reward circuits during hunger: a pilot fMRI study. *Obesity* 1566–1571. <https://doi.org/10.1038/oby.2010.57>.
- Carnell, S., Gibson, C., Benson, L., Ochner, C.N., Geliebter, A., 2012. Neuroimaging and obesity: current knowledge and future directions. *Obes. Rev.* 13, 43–56. <https://doi.org/10.1111/j.1467-789X.2011.00927.x>.
- Cauda, F., Costa, T., Torta, D.M.E., Sacco, K., D'agata, F., Duca, S., Geminiani, G., Fox, P.T., Vercelli, A., 2012. Meta-analytic clustering of the insular cortex: characterizing the meta-analytic connectivity of the insula when involved in active tasks. *Neuroimage* 62, 343–355. <https://doi.org/10.1016/j.neuroimage.2012.04.012>.
- Cauda, F., D'Agata, F., Sacco, K., Duca, S., Geminiani, G., Vercelli, A., 2011. Functional connectivity of the insula in the resting brain. *Neuroimage* 55, 8–23. <https://doi.org/10.1016/j.neuroimage.2010.11.049>.
- Chang, L.J., Yarkoni, T., Khaw, M.W., Sanfey, A.G., 2013. Decoding the role of the insula in human cognition: functional parcellation and large-scale reverse inference. *Cerebr. Cortex* 23, 739–749. <https://doi.org/10.1093/cercor/bhs065>.
- Chodkowski, B.A.A., Cowan, R.L., Niswender, K.D., 2016. Imbalance in resting state functional connectivity is associated with eating behaviors and adiposity in children. *Heliyon* 2, 58. <https://doi.org/10.1016/j.heliyon.2015.e00058>.
- Clayton, D.J., Creese, M., Skidmore, N., Stensel, D.J., James, L.J., 2016. No effect of 24 h severe energy restriction on appetite regulation and ad libitum energy intake in overweight and obese males. *Int. J. Obes.* 40, 1662–1670. <https://doi.org/10.1038/ijo.2016.106>.
- Craig, A.D., 2014. *How Do You Feel?: an Interoceptive Moment with Your Neurobiological Self*. Princeton University Press.
- Craig, A.D., 2009. How do you feel — now? The anterior insula and human awareness. *Nat. Rev. Neurosci.* 10, 59–70. <https://doi.org/10.1038/nrn2555>.
- Craig, A.D.B., 2005. Forebrain emotional asymmetry: a neuroanatomical basis?, 9 *Trends in cognitive sciences*, pp. 566–571.
- Dagher, A., Han, J.-E., Neseliler, S., 2017. The use of functional magnetic resonance imaging in the study of appetite and obesity. In: *Appetite and Food Intake*. CRC Press, pp. 117–134.
- Daunizeau, J., David, O., Stephan, K.E., 2011. Dynamic causal modelling: a critical review of the biophysical and statistical foundations. *Neuroimage* 58, 312–322. <https://doi.org/10.1016/j.neuroimage.2009.11.062>.
- De Silva, A., Salem, V., Matthews, P.M., Dhillo, W.S., 2012. The use of functional MRI to study appetite control in the CNS. *Exp. Diabetes Res.* <https://doi.org/10.1155/2012/764017>, 2012.
- DelParigi, A., Chen, K., Salbe, A.D., Reiman, E.M., Tataranni, P.A., 2005. Sensory experience of food and obesity: a positron emission tomography study of the brain regions affected by tasting a liquid meal after a prolonged fast. *Neuroimage* 24, 436–443. <https://doi.org/10.1016/j.neuroimage.2004.08.035>.
- Druce, M.R., Small, C.J., Bloom, S.R., 2004. Minireview: gut peptides regulating satiety. *Endocrinology* 145, 2660–2665. <https://doi.org/10.1210/en.2004-0089>.
- Frank, P., Katz, A., Andersson, E., Sahlin, K., 2013. Acute exercise reverses starvation-mediated insulin resistance in humans. *Am. J. Physiol. Metab.* 304, E436–E443. <https://doi.org/10.1152/ajpendo.00416.2012>.
- Frank, S., Kullmann, S., Veit, R., 2013. Food related processes in the insular cortex. *Front. Hum. Neurosci.* 7, 1–6. <https://doi.org/10.3389/fnhum.2013.00499>.
- Friston, K., 2005. A theory of cortical responses. *Philos. Trans. R. Soc. B Biol. Sci.* 360, 815–836. <https://doi.org/10.1098/rstb.2005.1622>.
- Friston, K., Kahan, J., Biswal, B., Razi, A., 2014. A DCM for resting state fMRI. *Neuroimage* 94, 396–407. <https://doi.org/10.1016/j.neuroimage.2013.12.009>.
- Friston, K.J., Harrison, L., Penny, W., 2003. Dynamic causal modelling. *Neuroimage* 19, 1273–1302. [https://doi.org/10.1016/S1053-8119\(03\)00202-7](https://doi.org/10.1016/S1053-8119(03)00202-7).
- Friston, K.J., Li, B., Daunizeau, J., Stephan, K.E., 2011. Network discovery with DCM. *Neuroimage* 56, 1202–1221. <https://doi.org/10.1016/j.neuroimage.2010.12.039>.
- Friston, K.J., Williams, S., Howard, R., Frackowiak, R.S.J., Turner, R., 1996. Movement-related effects in fMRI time-series. *Magn. Reson. Med.* 35, 346–355. <https://doi.org/10.1002/mrm.1910350312>.
- Galecki, A., Burzykowski, T., 2013. *Linear Mixed-Effects Models Using R: A Step-by-step Approach*. Springer Texts in Statistics, New York.
- Haase, L., Green, E., Murphy, C., 2011. Males and females show differential brain activation to taste when hungry and sated in gustatory and reward areas. *Appetite* 57, 421–434. <https://doi.org/10.1016/j.appet.2011.06.009>.
- Johnstone, A.M., Faber, P., Andrew, R., Gibney, E.R., Elia, M., Lobley, G., Stubbs, R.J., Walker, B.R., 2004. Influence of short-term dietary weight loss on cortisol secretion and metabolism in obese men. *Eur. J. Endocrinol.* 150, 185–194. <https://doi.org/10.1530/eje.0.1500185>.
- Kann, S., Zhang, S., Manza, P., Leung, H.-C., Li, C.-S.R., 2016. Hemispheric lateralization of resting-state functional connectivity of the anterior insula: association with age, gender, and a novelty-seeking trait. *Brain Connect.* 6, 724–734. <https://doi.org/10.1089/brain.2016.0443>.
- Kullmann, S., Frank, S., Heni, M., Ketterer, C., Veit, R., Häring, H.-U., Fritsche, A., Preissl, H., 2013. Intra-nasal insulin modulates intrinsic reward and prefrontal circuitry of the human brain in lean women. *Neuroendocrinology* 97, 176–182. <https://doi.org/10.1159/000341406>.
- Kullmann, S., Heni, M., Linder, K., Zipfel, S., Häring, H., Veit, R., Fritsche, A., Preissl, H., 2014. Resting-state functional connectivity of the human hypothalamus. *Hum. Brain Mapp.* 35, 6088–6096. <https://doi.org/10.1002/hbm.22607>.
- Kullmann, S., Heni, M., Veit, R., Ketterer, C., Schick, F., Häring, H.U., Fritsche, A., Preissl, H., 2012b. The obese brain: association of body mass index and insulin sensitivity with resting state network functional connectivity. *Hum. Brain Mapp.* 33, 1052–1061. <https://doi.org/10.1002/hbm.21268>.
- Lemaire, J.-J., Frew, A.J., McArthur, D., Gorgulho, A.A., Alger, J.R., Salomon, N., Chen, C., Behne, E.J., De Salles, A.A.F., 2011. White matter connectivity of human hypothalamus. *Brain Res.* 1371, 43–64. <https://doi.org/10.1016/j.brainres.2010.11.072>.
- Lips, M.A., Wijngaarden, M.A., Van Der Grond, J., Van Buchem, M.A., De Groot, G.H., Rombouts, S.A.R.B., Pijl, H., Veer, I.M., 2014. Resting-state functional connectivity of brain regions involved in cognitive control, motivation, and reward is enhanced in obese females. *Am. J. Clin. Nutr.* 100, 524–531. <https://doi.org/10.3945/ajcn.113.080671>.
- Little, T.J., McKie, S., Jones, R.B., D'Amato, M., Smith, C., Kiss, O., Thompson, D.G., McLaughlin, J.T., 2014. Mapping glucose-mediated gut-to-brain signalling pathways in humans. *Neuroimage* 96, 1–11. <https://doi.org/10.1016/j.neuroimage.2014.03.059>.
- Lizarte, B., Benitez, A., Peláez Brioso, G.A., Sánchez-Montañés, M., López-Larrubia, P., Ballesteros, P., Cerdán, S., 2013. Hypothalamic metabolic compartmentation during appetite regulation as revealed by magnetic resonance imaging and spectroscopy methods. *Front. Neuroenergetics* 5, 1–14. <https://doi.org/10.3389/fnene.2013.00006>.
- Lüdtke, D., 2018. sjPlot: data visualization for statistics in social science. R package version 2.6.1 [WWW Document]. <https://cran.r-project.org/web/packages/sjPlot/index.html>.
- Manjaly, Z.M., Harrison, N.A., Critchley, H.D., Do, C.T., Stefanics, G., Wenderoth, N., et al., 2019. Pathophysiological and cognitive mechanisms of fatigue in multiple sclerosis. *J. Neurol. Neurosurg. Psychiatr.* 90, 642–651. <https://doi.org/10.1136/jnnp-2018-320050>.
- Maldjian, J.A., Laurienti, P.J., Kraft, R.A., Burdette, J.H., 2003. An automated method for neuroanatomic and cytoarchitectonic atlas-based interrogation of fMRI data sets. *Neuroimage* 19, 1233–1239. [https://doi.org/10.1016/S1053-8119\(03\)00169-1](https://doi.org/10.1016/S1053-8119(03)00169-1).
- Marić, G., Gazibara, T., Zaletel, I., Borović, M.L., Tomanović, N., 2014. The role of gut hormones in appetite regulation. *Review* 101, 395–407. <https://doi.org/10.1556/APHysiol.101.2014.4.1>.
- Mayer, E.A., 2011. Gut feelings: the emerging biology of gut–brain communication. *Nat. Rev. Neurosci.* 12, 453–466. <https://doi.org/10.1038/nrn3071>.
- Mayer, J., Thomas, D.W., 1967. Regulation of food intake and obesity. *Science* 165, 328–337. <https://doi.org/10.1126/science.156.3773.328>.
- McGuire, P.K., Bates, J.F., Goldman-Rakic, P.S., 1991. Interhemispheric integration: II. Symmetry and convergence of the corticostriatal projections of the left and the right principal sulcus (PS) and the left and the right supplementary motor area (SMA) of the rhesus monkey. *Cerebr. Cortex*. <https://doi.org/10.1093/cercor/1.5.408>.
- Moreno-Lopez, L., Contreras-Rodriguez, O., Soriano-Mas, C., Stamatakis, E.A., Verdejo-García, A., 2016. Disrupted functional connectivity in adolescent obesity. *Neuroimage Clin* 12, 262–268. <https://doi.org/10.1016/j.nicl.2016.07.005>.
- Morton, G.J., Meek, T.H., Schwartz, M.W., 2014. Neurobiology of food intake in health and disease. *Nat. Rev. Neurosci.* 15, 367–378. <https://doi.org/10.1038/nrn3745>.
- Murray, S., Tulloch, A., Gold, M.S., Avena, N.M., 2014. Hormonal and neural mechanisms of food reward, eating behaviour and obesity. *Nature Reviews Endocrinology* 10, 540–552. <https://doi.org/10.1038/nrendo.2014.91>.
- Ojemann, J.G., Akbudak, E., Snyder, A.Z., McKinsty, R.C., Raichle, M.E., Conturo, T.E., 1997. Anatomic localization and quantitative analysis of gradient refocused echoplanar fMRI susceptibility artifacts. *Neuroimage* 6, 156–167. <https://doi.org/10.1006/nimg.1997.0289>.
- Pelchat, M.L., Johnson, A., Chan, R., Valdez, J., Ragland, J.D., 2004. Images of desire: food-craving activation during fMRI. *Neuroimage* 23, 1486–1493. <https://doi.org/10.1016/j.neuroimage.2004.08.023>.
- Penfield, W., Faulk, M.E., 1955. The insula: further observations on its function. *Brain* 78, 445–470. <https://doi.org/10.1093/brain/78.4.445>.
- Penny, W.D., Stephan, K.E., Mechelli, A., Friston, K.J., 2004. Comparing dynamic causal models. *Neuroimage* 22, 1157–1172. <https://doi.org/10.1016/j.neuroimage.2004.03.026>.
- Pezzulo, G., Rigoli, F., Friston, K., 2015. Active Inference, homeostatic regulation and adaptive behavioural control. *Prog. Neurobiol.* 134, 17–35. <https://doi.org/10.1016/j.pneurobio.2015.09.001>.
- Pitt, M.A., Myung, I.J., 2002. When a good fit can be bad. *Trends Cognit. Sci.* 6, 421–425. [https://doi.org/10.1016/s1364-6613\(02\)01964-2](https://doi.org/10.1016/s1364-6613(02)01964-2).
- Purnell, J.Q., Lahna, D.L., Samuels, M.H., Rooney, W.D., Hoffman, W.F., 2014. Loss of pons-to-hypothalamic white matter tracks in brainstem obesity. *Int. J. Obes.* 38, 1573–1577. <https://doi.org/10.1038/ijo.2014.57>.
- Rao, R.P.N., Ballard, D.H., 1999. Predictive coding in the visual cortex: a functional interpretation of some extra-classical receptive-field effects. *Nat. Neurosci.* 2, 79–87. <https://doi.org/10.1038/4580>.
- Razi, A., Friston, K.J., 2016. The connected brain: causality, models, and intrinsic dynamics. *IEEE Signal Process. Mag.* 33, 14–35. <https://doi.org/10.1109/MSP.2015.2482121>.
- Razi, A., Kahan, J., Rees, G., Friston, K.J., 2015. Construct validation of a DCM for resting state fMRI. *Neuroimage* 106, 1–14. <https://doi.org/10.1016/j.neuroimage.2014.11.027>.
- Rolls, E.T., 2006. Brain mechanisms underlying flavour and appetite. *Philos. Trans. R. Soc. Lond. B Biol. Sci.* 361, 1123–1136. <https://doi.org/10.1098/rstb.2006.1852>.
- Schloegl, H., Percik, R., Horstmann, A., Villringer, A., Stumvoll, M., 2011. Peptide hormones regulating appetite—focus on neuroimaging studies in humans. *Diabetes. Metab. Res. Rev.* 27, 104–112. <https://doi.org/10.1002/dmrr.1154>.
- Schweinhart, P., Glynn, C., Brooks, J., McQuay, H., Jack, T., Chessell, I., Bountra, C., Tracey, I., 2006. An fMRI study of cerebral processing of brush-evoked allodynia in

- neuropathic pain patients. *Neuroimage* 32, 256–265. <https://doi.org/10.1016/j.neuroimage.2006.03.024>.
- Seth, A.K., Suzuki, K., Critchley, H.D., 2012. An interoceptive predictive coding model of conscious presence. *Front. Psychol.* 2, 1–16. <https://doi.org/10.3389/fpsyg.2011.00395>.
- Seth, A.K., 2013. Interoceptive inference, emotion, and the embodied self. *Trends Cognit. Sci.* 17, 565–573. <https://doi.org/10.1016/j.tics.2013.09.007>.
- Sladky, R., Friston, K.J., Tr??stl, J., Cunnington, R., Moser, E., Windischberger, C., 2011. Slice-timing effects and their correction in functional MRI. *Neuroimage* 58, 588–594. <https://doi.org/10.1016/j.neuroimage.2011.06.078>.
- Smeets, P. a M., Vidarsdottir, S., de Graaf, C., Stafleu, A., van Osch, M.J.P., Viergever, M. a, Pijl, H., van der Grond, J., 2007. Oral glucose intake inhibits hypothalamic neuronal activity more effectively than glucose infusion. *Am. J. Physiol. Endocrinol. Metab.* 293, E754–E758. <https://doi.org/10.1152/ajpendo.00231.2007>.
- Smeets, P.A.M., De Graaf, C., Stafleu, A., Van Osch, M.J.P., Van Der Grond, J., 2005. Functional MRI of human hypothalamic responses following glucose ingestion. *Neuroimage* 24, 363–368. <https://doi.org/10.1016/j.neuroimage.2004.07.073>.
- Stephan, K.E., Friston, K.J., 2010. Analyzing effective connectivity with functional magnetic resonance imaging. *Wiley Interdiscip. Rev. Cogn. Sci.* 1, 446–459. <https://doi.org/10.1002/wcs.58>.
- Stephan, K.E., Manjaly, Z.M., Mathys, C.D., Weber, L.A.E., Paliwal, S., Gard, T., Tittgemeyer, M., Fleming, S.M., Haker, H., Seth, A.K., Petzschner, F.H., 2016. Allostatic self-efficacy: a metacognitive theory of dyshomeostasis-induced fatigue and depression. *Front. Hum. Neurosci.* 10, 1–27. <https://doi.org/10.3389/fnhum.2016.00550>.
- Stephan, K.E., Marshall, J.C., Penny, W.D., Friston, K.J., Fink, G.R., 2007. Interhemispheric integration of visual processing during task-driven lateralization. *J. Neurosci.* 27, 3512–3522. <https://doi.org/10.1523/JNEUROSCI.4766-06.2007>.
- Stephan, K.E., Penny, W.D., Daunizeau, J., Moran, R.J., Friston, K.J., 2009. Bayesian model selection for group studies. *Neuroimage* 46, 1004–1017. <https://doi.org/10.1016/j.neuroimage.2009.03.025>.
- Stephan, K.E., Penny, W.D., Moran, R.J., den Ouden, H.E.M., Daunizeau, J., Friston, K.J., 2010. Ten simple rules for dynamic causal modeling. *Neuroimage* 49, 3099–3109. <https://doi.org/10.1016/j.neuroimage.2009.11.015>.
- Sun, T., Hevner, R.F., 2014. Growth and folding of the mammalian cerebral cortex: from molecules to malformations. *Nat. Rev. Neurosci.* 15, 217–232. <https://doi.org/10.1038/nrn3707>.
- Suzuki, K., Simpson, K.A., Minnion, J.S., Shillito, J.C., Bloom, S.R., 2010. The role of gut hormones and the hypothalamus in appetite regulation, 57. *Endocrine Journal*, pp. 359–372.
- Thomas, J.M., Higgs, S., Dourish, C.T., Hansen, P.C., Harmer, C.J., McCabe, C., 2015. Satiety attenuates BOLD activity in brain regions involved in reward and increases activity in dorsolateral prefrontal cortex: an fMRI study in healthy volunteers. *Am. J. Clin. Nutr.* 101, 697–704. <https://doi.org/10.3945/ajcn.114.097543>.
- Timper, K., Br??ning, J.C., 2017. Hypothalamic circuits regulating appetite and energy homeostasis: pathways to obesity. *DMM Dis. Model. Mech.* 10, 679–689. <https://doi.org/10.1242/dmm.026609>.
- Tomiyama, A.J., Mann, T., Vinas, D., Hunger, J.M., DeJager, J., Taylor, S.E., 2010. Low calorie dieting increases cortisol. *Psychosom. Med.* 72, 357–364. <https://doi.org/10.1097/PSY.0b013e3181d9523c>.
- Val-Laillet, D., Aarts, E., Weber, B., Ferrarri, M., Quaresima, V., Stoeckel, L.E., Alonso-Alonso, M., Audette, M., Malbert, C.H., Stice, E., 2015. Neuroimaging and neuromodulation approaches to study eating behavior and prevent and treat eating disorders and obesity. *NeuroImage Clin* 8, 1–31. <https://doi.org/10.1016/j.nicl.2015.03.016>.
- Valassi, E., Scacchi, M., Cavagnini, F., 2008. Neuroendocrine control of food intake. *Nutr. Metabol. Cardiovasc. Dis.* 18, 158–168. <https://doi.org/10.1016/j.numecd.2007.06.004>.
- Wang, G.J., Tomasi, D., Backus, W., Wang, R., Telang, F., Geliebter, A., Korner, J., Bauman, A., Fowler, J.S., Thanos, P.K., Volkow, N.D., 2008. Gastric distention activates satiety circuitry in the human brain. *Neuroimage* 39, 1824–1831. <https://doi.org/10.1016/j.neuroimage.2007.11.008>.
- Wijngaarden, M.A., Veer, I.M., Rombouts, S.A.R.B., Buchem, M.A. Van, Dijk, K.W. Van, Pijl, H., Grond, J. Van Der, 2015. Obesity is marked by distinct functional connectivity in brain networks involved in food reward and salience. *Behav. Brain Res.* 287, 127–134. <https://doi.org/10.1016/j.bbr.2015.03.016>.
- Woods, S.C., 2009. The control of food intake: behavioral versus molecular perspectives. *Cell Metabol.* 9, 489–498. <https://doi.org/10.1016/j.cmet.2009.04.007>.
- Woods, S.C., Ramsay, D.S., 2011. Food intake, metabolism and homeostasis. *Physiol. Behav.* 104, 4–7. <https://doi.org/10.1016/j.physbeh.2011.04.026>.
- Wright, H., Li, X., Fallon, N.B., Crookall, R., Giesbrecht, T., Thomas, A., Halford, J.C.G., Harrold, J., Stancak, A., 2016. Differential effects of hunger and satiety on insular cortex and hypothalamic functional connectivity. *Eur. J. Neurosci.* 43, 1181–1189. <https://doi.org/10.1111/ejn.13182>.
- Zanchi, D., Depoorter, A., Eglhoff, L., Haller, S., M??hlmann, L., Lang, U.E., Drewe, J., Beglinger, C., Schmidt, A., Borgwardt, S., 2017. The impact of gut hormones on the neural circuit of appetite and satiety: a systematic review. *Neurosci. Biobehav. Rev.* 80, 457–475. <https://doi.org/10.1016/j.neubiorev.2017.06.013>.
- American Diabetes Association, 2020. 2. Classification and diagnosis of diabetes: standards of medical care in diabetes. *Diabetes Care* 43.Suppl. 1: S14–S31.